JACS
JOURNAL OF THE AMERICAN CHEMICAL SOCIETY
Article
Cite This: J. Am. Chem. Soc. 2018, 140, 10324−10331
pubs.acs.org/JACS

Near-Perfect CO_2/CH_4 Selectivity Achieved through Reversible Guest Templating in the Flexible Metal−Organic Framework Co(bdp)

Mercedes K. Taylor,[†,‡] Tomče Runčevski,[†,‡] Julia Oktawiec,[†] Jonathan E. Bachman,[§] Rebecca L. Siegelman,[†,‡] Henry Jiang,[†] Jarad A. Mason,[†] Jacob D. Tarver,[∥,⊥] and Jeffrey R. Long*[,†,‡,§]

[†]Department of Chemistry, University of California, Berkeley, California 94720, United States
[‡]Materials Sciences Division, Lawrence Berkeley National Laboratory, Berkeley, California 94720, United States
[§]Department of Chemical and Biomolecular Engineering, University of California, Berkeley, California 94720, United States
[∥]NIST Center for Neutron Research, National Institute of Standards and Technology, Gaithersburg, Maryland 20899, United States
[⊥]National Renewable Energy Laboratory, Golden, Colorado 80401, United States

Supporting Information

ABSTRACT: Metal−organic frameworks are among the most promising materials for industrial gas separations, including the removal of carbon dioxide from natural gas, although substantial improvements in adsorption selectivity are still sought. Herein, we use equilibrium adsorption experiments to demonstrate that the flexible metal−organic framework Co(bdp) (bdp^{2-} = 1,4-benzenedipyrazolate) exhibits a large CO_2 adsorption capacity and approaches complete exclusion of CH_4 under 50:50 mixtures of the two gases, leading to outstanding CO_2/CH_4 selectivity under these conditions. *In situ* powder X-ray diffraction data indicate that this selectivity arises from reversible guest templating, in which the framework expands to form a CO_2 clathrate and then collapses to the nontemplated phase upon desorption. Under an atmosphere dominated by CH_4, Co(bdp) adsorbs minor amounts of CH_4 along with CO_2, highlighting the importance of studying all relevant pressure and composition ranges via multicomponent measurements when examining mixed-gas selectivity in structurally flexible materials. Altogether, these results show that Co(bdp) may be a promising CO_2/CH_4 separation material and provide insights for the further study of flexible adsorbents for gas separations.

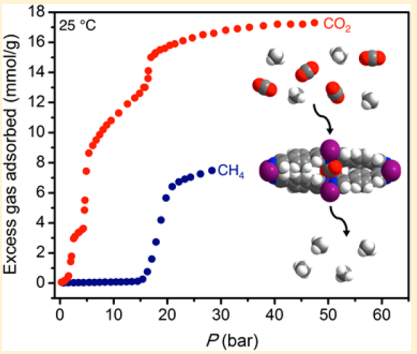

INTRODUCTION

Industrial separations are a major source of global energy demand and greenhouse gas emissions, currently comprising ∼15% of the total U.S. energy consumption.[1] The separation of CO_2 from CH_4 is of particular importance due to the widespread and increasing use of natural gas as a fuel.[2] Highly selective adsorbents that exhibit reversible gas uptake could significantly reduce the energy spent on gas separations,[3] but the design of porous adsorbents that completely exclude one species while showing high capacities for another is difficult when considering mixtures of adsorbate molecules with similar sizes and properties.

Due to their high internal surface areas and tunable pore architectures, metal−organic frameworks are regarded as a particularly promising class of adsorbents for gas separation applications,[4] and some frameworks additionally exhibit structural flexibility that allows them to undergo reversible phase changes in response to external stimuli such as gas pressure.[5] Adsorbate-induced phase changes typically manifest as steep steps in adsorption isotherms, and these steps can occur at different pressures, depending on the adsorbate. Because of this unique adsorption behavior, flexible metal−organic frameworks have garnered increasing attention as possible gas separation materials.[6] However, while single-component adsorption isotherms for these materials may suggest selectivity for a given gas within a certain pressure range, very few studies have carried out the necessary multicomponent equilibrium adsorption experiments to confirm selectivity and demonstrate that it arises from adsorbate-dependent expansion.[6g,i,l] Much therefore remains unknown about this separation mechanism in flexible frameworks, such as whether pore opening induced by one molecule will then enable the simultaneous uptake of other molecules. Assuming this simultaneous uptake does not occur, it is then unknown whether selectivity arising in a region where only one gas induces a phase change (e.g., the region highlighted in gray in Figure 1b) will persist beyond subsequent steps in the respective single-component isotherms, and under what conditions the adsorption selectivity may be lost.

We sought to address these unknowns by studying the CO_2/CH_4 separation performance of the metal−organic framework Co(bdp) (bdp^{2-} = 1,4-benzenedipyrazolate). This framework exhibits significant structural flexibility under increasing gas pressure, undergoing endothermic structural phase changes in response to adsorption, and shows one of the highest CH_4

Received: June 8, 2018
Published: July 22, 2018

Downloaded via UNIV OF CALIFORNIA BERKELEY on August 25, 2018 at 22:24:22 (UTC).
See https://pubs.acs.org/sharingguidelines for options on how to legitimately share published articles.

© 2018 American Chemical Society

DOI: 10.1021/jacs.8b06062
J. Am. Chem. Soc. 2018, 140, 10324−10331

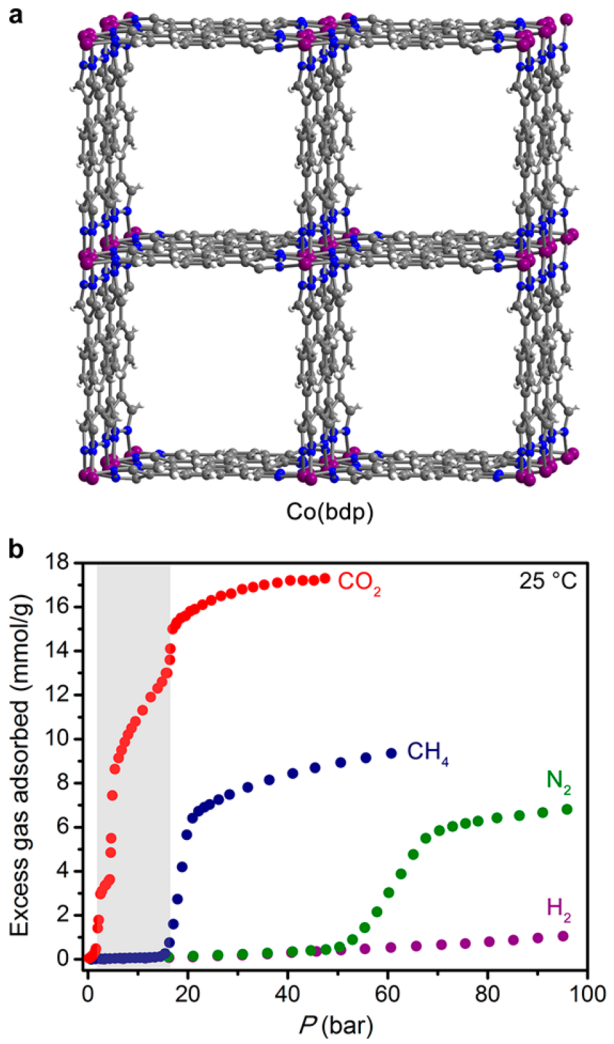

Figure 1. (a) Single-crystal X-ray diffraction structure at 298 K of the diethylformamide-solvated, fully expanded phase of Co(bdp) showing the one-dimensional square channels of this material, which are bounded by rows of organic ligands and chains of tetrahedral cobalt(II) centers.[7d] Solvent molecules in the framework pores are not depicted. Gray, blue, white, and purple spheres represent C, N, H, and Co atoms, respectively. (b) Single-component isotherms for CO_2, CH_4, N_2, and H_2 adsorption in Co(bdp) at 25 °C showing adsorbate-dependent phase change pressures. The isotherms suggest that Co(bdp) exhibits perfect CO_2/CH_4 selectivity within the gray highlighted region, a hypothesis examined with multicomponent adsorption experiments in this work. Desorption data and variable-temperature isotherm data are provided in the Supporting Information.

capacities to date.[7] Composed of coordinatively saturated, tetrahedral cobalt(II) centers linked by bdp^{2-} ligands (Figure 1a), Co(bdp) contains no open metal sites and is completely nonporous to gases in its collapsed phase, traits which simplify the interpretation of adsorption data and facilitate an unhindered investigation into the effect of structural phase changes on adsorption selectivities. Herein, we use multicomponent equilibrium adsorption measurements supplemented with *in situ* powder X-ray diffraction analyses to demonstrate high CO_2/CH_4 selectivity in Co(bdp) and to probe the limits of this selectivity.

EXPERIMENTAL SECTION

Synthesis. Co(bdp) and Co(F-bdp) were synthesized according to previously published procedures;[7c,d] synthetic details are provided in the Supporting Information.

Single-Component Gas Adsorption Experiments. Ultrahigh purity (≥99.998% purity) dinitrogen, helium, carbon dioxide, methane, and dihydrogen were used for all adsorption measurements. Adsorption isotherms for pressures in the range 0−1.1 bar were measured using a Micromeritics ASAP 2020 or 2420 gas adsorption analyzer. Activated samples were transferred under a N_2 atmosphere to preweighed analysis tubes, which were capped with a Transeal. Each sample was evacuated on the instrument until the outgas rate was less than 3 μbar/min. The evacuated analysis tube containing degassed sample was then transferred to an electronic balance and weighed to determine the mass of sample (typically 30−50 mg). For cryogenic measurements, the tube was fitted with an isothermal jacket. The tube was then transferred back to the analysis port of the instrument, and the outgas rate was again confirmed to be less than 3 μbar/min prior to analysis.

Adsorption isotherms for pressures in the range 0−100 bar were measured on an HPVA-II-100 gas adsorption analyzer from Particulate Systems, a Micromeritics company. In a typical measurement, 0.2−0.5 g of activated sample was loaded into a tared stainless steel sample holder inside a glovebox under a N_2 atmosphere. The sample holder was weighed to determine the sample mass and was then connected to the high-pressure assembly inside the glovebox. The sample holder was then transferred to the HPVA-II-100, connected to the analysis port of the instrument via an OCR fitting, and evacuated at room temperature for at least 2 h. The sample holder was then placed inside an aluminum recirculating dewar connected to a Julabo FP89-HL isothermal bath filled with Sylthern XLT fluid. The temperature stability of the isothermal bath was ±0.02 °C. Methods for accurately measuring the relevant sample freespaces, involving the expansion of He from a calibrated volume at 0.7 bar and 25 °C to the evacuated sample holder, have been described in detail previously.[8] Nonideality corrections were performed using the compressibility factor of the appropriate gas, tabulated in the NIST REFPROP database,[9] for each measured temperature and pressure.

Multicomponent Gas Adsorption Experiments. Premixed cylinders containing 50:50 and 10:90 CO_2/CH_4 gas mixtures were purchased from Praxair with an analytical accuracy of ±1%. Co(bdp) was dosed with one of the gas mixtures using the HPVA-II-100 instrument as described above and allowed to reach equilibrium, as evidenced by a pressure change of less than 0.003 bar over 2 min. The gas pressure of the manifold was recorded before and after equilibration (as is done for each point of a single-component isotherm). After taking each data point, the sample holder was sealed without desorbing the gas from the sample, removed from the HPVA-II-100, and attached to an evacuated volume. The gas mixture in the headspace of the sample holder as well as the gas adsorbed on the sample was expanded into the evacuated volume by heating the sample holder to 160 °C for 1 h. The gas mixture was then sampled with a mass spectrometer (MKS Microvision 2) to determine the relative concentrations of CO_2 and CH_4 that were present in the sample holder upon removal from the HPVA-II-100 instrument. Using the free-space and adsorption data provided by the HPVA-II-100 instrument, the CO_2/CH_4 ratio obtained from the mass spectrometer was used to calculate the amount of CO_2 and CH_4 adsorbed by Co(bdp). A complete discussion of these calculations is presented in the Supporting Information.

***In Situ* Powder X-ray Diffraction Experiments.** High-resolution powder X-ray diffraction patterns were collected for Co(bdp) at Beamline 17-BM-B at the Advanced Photon Source of Argonne National Laboratory, with an average wavelength ranging from 0.4 to 0.7 Å. Scattered intensity was recorded by a PerkinElmer a-Si Flat Panel detector. Prior to measurement, samples were packed in quartz glass capillaries of 1.5 mm diameter under a N_2 atmosphere. Each capillary was attached to a custom-designed gas-dosing cell equipped with a gas valve, which was then mounted onto the

DOI: 10.1021/jacs.8b06062
J. Am. Chem. Soc. 2018, 140, 10324−10331

goniometer head and connected to a gas-dosing manifold for *in situ* diffraction measurements. First, diffraction data were collected at room temperature under dynamic vacuum to obtain the structure of the material in the collapsed phase. Subsequently, the gas-dosing manifold was used to dose increasing pressures of pure CO_2, and diffraction data were collected after the sample reached equilibrium at each pressure (as evidenced by a constant pressure readout and unchanging diffraction pattern). The sample was then evacuated to regenerate the collapsed phase and subsequently dosed with increasing pressures of a 50:50 mixture of CO_2/CH_4. Diffraction data were again collected after the sample reached equilibrium at each mixed-gas pressure. A sample temperature of 298 K was maintained for all measurements by an Oxford CryoSystems Cryostream 800. Analysis of all diffraction data is discussed in the Supporting Information.

RESULTS AND DISCUSSION

Single-Component Gas Adsorption Behavior. Single-component CO_2, CH_4, N_2, and H_2 adsorption isotherms were collected for Co(bdp) at 25 °C and are shown in Figure 1b (CO_2 and CH_4 isotherms at 25 °C for Co(bdp) have been reported previously;[7b,c] variable-temperature isotherm data are provided in the Supporting Information). These isotherms illustrate that phase changes in Co(bdp) occur at markedly different pressures for different adsorbates: the first phase change (from a nonporous, collapsed structure to a porous, expanded structure) occurs at ~2 bar for CO_2 but not until 18 bar for CH_4 and 60 bar for N_2. While H_2 has been found to induce phase changes in Co(bdp) at cryogenic temperatures,[7a] no phase change was observed below 100 bar for H_2 at 25 °C. Although the phase change pressure is influenced by a number of thermodynamic parameters, the relative position of the steps in the CO_2, CH_4, N_2, and H_2 isotherms can be explained in part by the relative binding enthalpies of these gases: Stronger-binding gases like CO_2 provide more energetic stabilization for the expanded phase, so less gas pressure is necessary to trigger the expansion.[10] The wide variation in phase change pressures implies that Co(bdp) has the potential to be used for numerous separations involving CO_2, CH_4, N_2, and H_2, including in the industrially important processes of natural gas sweetening,[11] hydrogen production,[12] and biogas purification.[13] We chose to focus our characterization efforts on the removal of CO_2 from mixtures with CH_4 because of the industrial relevance of this separation, because both the CO_2- and CH_4-induced phase change pressures are compatible with a variety of adsorption and diffraction experiments, and because of the notably high CO_2 capacity of Co(bdp).[14]

Equilibrium Multicomponent Adsorption Experiments. Comparison of the CO_2 and CH_4 single-component adsorption isotherms in Figure 1b suggests that Co(bdp) would be highly selective for CO_2 at pressures below those corresponding to the CH_4-induced phase change. However, calculating noncompetitive selectivities for CO_2 and CH_4 from these data would erroneously exclude the possibility that Co(bdp) could expand to a novel phase capable of then accommodating a mixture of CO_2 and CH_4 molecules in the pores. Furthermore, using ideal adsorbed solution theory to model mixed-gas isotherms (as is often done for rigid frameworks) is inappropriate for structurally flexible materials such as Co(bdp),[7c] because this theory assumes that the thermodynamic state of the adsorbent remains constant during adsorption.[15] While progress has been made in developing a more representative computational method to predict mixed-gas selectivity in flexible metal−organic frameworks from their pure-gas isotherms,[16] the most thorough way to experimentally determine a flexible framework's selectivity is to perform multicomponent adsorption experiments, in which a sample is exposed to the relevant gas mixture. However, when multicomponent selectivity is reported in the literature, it is usually as the result of the dynamic breakthrough measurements.[17] The results of breakthrough experiments depend on many factors in addition to the inherent properties of the adsorbent, including gas flow rate, column size, shape, length, packing density, and extra-column effects,[18] whereas equilibrium adsorption measurements entail fewer experimental variables and are not subject to kinetic effects. As such, equilibrium measurements provide a more fundamental picture of adsorbent behavior and enable direct comparisons between materials.[19]

Therefore, we devised a multicomponent adsorption experiment that would allow us to study high-pressure, mixed-gas adsorption in Co(bdp) under equilibrium conditions. In brief, Co(bdp) was dosed with high pressures of a CO_2/CH_4 mixture and allowed to equilibrate at 25 °C, and mass spectrometry was then used to determine the composition of the adsorbed gas and the gas in the headspace (see the Supporting Information for further details). This experiment was performed for equilibrium pressures of 6.7, 13.9, and 25.3 bar, corresponding to equilibrium CO_2/CH_4 molar ratios of 46:54, 42:58, and 43:57, respectively (Figure 2a). For each examined pressure, the amount of CO_2 adsorbed coincides with the pure-CO_2 isotherm when plotted versus the equilibrium partial pressure of CO_2, while the amount of CH_4 adsorbed approaches zero for all cases. Thus, the hypothesis based on the single-component CO_2 and CH_4 isotherms is indeed correct, and under the conditions tested Co(bdp) has an outstanding CO_2/CH_4 selectivity. Because Co(bdp) adsorbs approximately no CH_4 at the examined pressures, calculated selectivity values are not meaningful, and the framework is most accurately described as having near-perfect CO_2 selectivity under these conditions.

***In Situ* Powder X-ray Diffraction with Mixed-Gas Dosing.** Synchrotron X-ray powder diffraction experiments were employed to further examine the phase behavior of Co(bdp) upon exposure to a mixture of CO_2 and CH_4. Data were first collected on an evacuated sample of the framework and confirmed that in this state Co(bdp) exhibits a collapsed structure identical to that previously published[7c] (Rietveld refinement results are provided in Figure S22). The activated sample was then dosed with increasing pressures of pure CO_2 from 0 to 19.4 bar in 0.5−2 bar increments, and X-ray diffraction data were collected at each pressure following sample equilibration, as evidenced by a lack of change in both pressure and the diffraction pattern (Figure 3a). After obtaining diffraction data for the highest pressure, the sample was evacuated to recover the collapsed phase, and a similar procedure was repeated with a 50:50 mixture of CO_2/CH_4 dosed at pressures ranging from 1.3 to 50 bar (Figure 3b).

A comparison of the diffraction patterns obtained after pure-CO_2 dosing with those obtained after CO_2/CH_4 dosing reveals these patterns to be strikingly similar at comparable CO_2 partial pressures (and distinct from the previously published CH_4-dosed diffraction patterns[7c]). Indeed, diffraction patterns collected for Co(bdp) equilibrated with 3.6 bar of pure CO_2 and with 7.2 bar of a 50:50 CO_2/CH_4 mixture (P_{CO_2} = 3.6 bar) were solved to yield identical structural models that represent

DOI: 10.1021/jacs.8b06062
J. Am. Chem. Soc. 2018, 140, 10324−10331

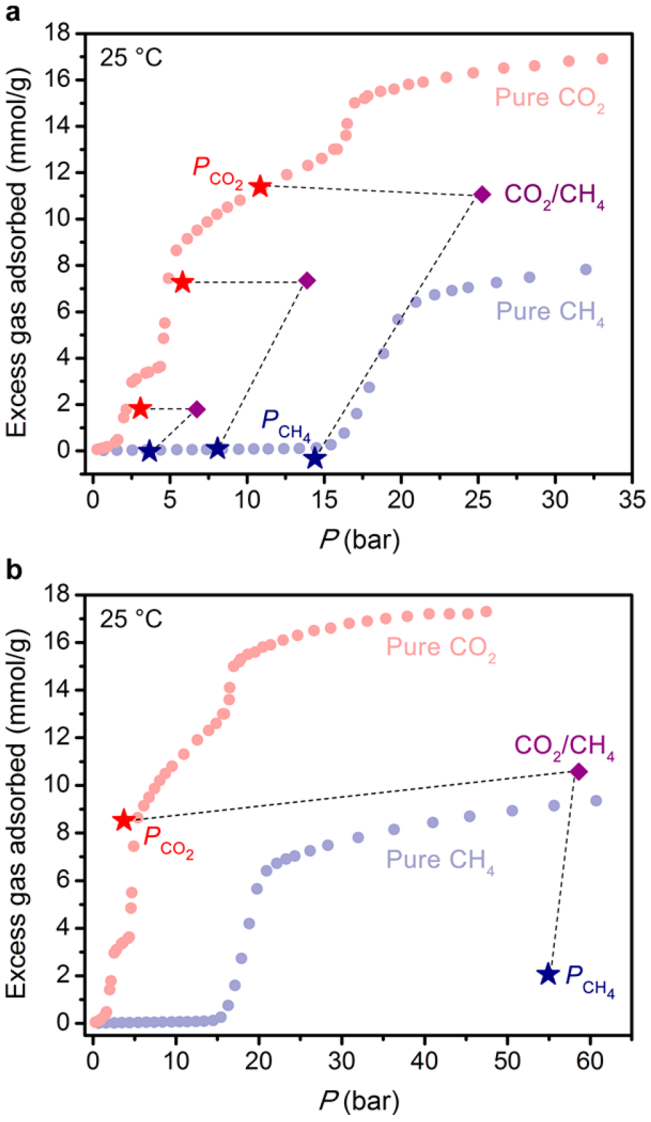

Figure 2. (a) Multicomponent adsorption experiments for CO_2/CH_4 mixtures in Co(bdp) show near-perfect CO_2 selectivity at 6.7, 13.9, and 25.3 bar, under equilibrium CO_2/CH_4 molar ratios of 46:54, 42:58, and 43:57, respectively. (b) Multicomponent adsorption experiment performed under a CH_4-rich atmosphere (with an equilibrium CO_2/CH_4 molar ratio of 6:94) shows that Co(bdp) adsorbs only a small amount of CH_4 at this ratio, leading to a selectivity of 61 ± 4. For (a) and (b), purple diamonds represent the overall amount of gas adsorbed by Co(bdp) (*y*-axis) from a CO_2/CH_4 mixture at a given equilibrium pressure (*x*-axis). Each purple diamond is paired with a corresponding red and blue star: red stars represent the CO_2 adsorbed from the mixture (*y*-axis) at the equilibrium partial pressure of CO_2 (*x*-axis), and blue stars represent the CH_4 adsorbed from the mixture (*y*-axis) at the equilibrium partial pressure of CH_4 (*x*-axis). Single-component isotherms of CO_2 (red circles) and CH_4 (blue circles) in Co(bdp) are shown for reference.

the phase giving rise to the first plateau in the pure-CO_2 adsorption isotherm (Figure 3d,e). The adsorbed gas molecules could be located in both structures and were identified and refined as CO_2 only. The complete exclusion of CH_4 can be understood by examining the size of the channels in this initial expanded phase of the framework, which opens just enough to accommodate a single CO_2 molecule per formula unit but no additional molecules of CO_2 or CH_4 (Figure 3e). This CO_2 adsorption behavior is reminiscent of hydrocarbon selectivity recently identified in a copper-based metal−organic framework, which behaves as an ideal molecular sieve with pores that are sized to adsorb acetylene while completely excluding ethylene.[20] Similarly, Co(bdp) can be considered as a CO_2-templated molecular sieve with flexibility that allows it to achieve pores sized for near-perfect CO_2 selectivity, since incorporation of an occasional, differently shaped methane molecule would destabilize many surrounding unit cells within the crystal. Importantly, this highly selective templating is reversible, and the collapsed nonporous phase can be regenerated upon CO_2 desorption. Upon increasing the dosed CO_2 partial pressures beyond the magnitudes associated with the first plateau in the pure-gas isotherm, the diffraction patterns undergo successive discrete changes associated with structural expansions of the framework. In between these discrete phase changes, which are marked by the sudden appearance of new diffraction peaks and the disappearance of others, Co(bdp) exhibits "breathing" behavior—i.e., a gradual expansion in response to increasing gas pressure. This framework breathing is evidenced by gradually shifting diffraction peaks, in contrast to the discrete phase changes described above (Figure 3a,b). These more subtle expansions are associated with shallow increases in the CO_2 adsorption capacity (for example, from 8.6 to 13.0 mmol/g over 5.4−16.5 bar in the pure CO_2 isotherm, Figure 1).

As the CO_2/CH_4-dosed material expands due to breathing and phase changes, the *in situ* diffraction patterns yield unit cell volumes that are similar to or greater than those of the previously reported CH_4-expanded phase of Co(bdp),[7c] indicating that the framework is sufficiently expanded to admit CH_4 molecules into the pores. For example, equilibration with 14.9 bar of the 50:50 CO_2/CH_4 mixture leads to an increase in unit cell volume from 1182.97(9) Å^3 in the nonporous phase[7c] to 2185.5(11) Å^3 (Pawley refinement provided in Figure S27), which is similar to that of the CH_4-expanded phase (2293.8(5) Å^3).[7c] In spite of its large unit cell volume, Co(bdp) continues to exhibit near-perfect CO_2/CH_4 selectivity in this pressure region, as evidenced by the 13.9 bar data point in Figure 2a. Consequently, the remarkable CO_2/CH_4 selectivity in this region can no longer be ascribed to size exclusion and instead likely arises due to the formation of a reversible CO_2-templated clathrate within the pores, with a packing arrangement that maximizes the van der Waals contacts between CO_2 molecules and the walls of the framework. The ability to form guest-specific clathrates, with pores templated around an optimal packing of identical guest molecules, confers a distinct advantage on highly flexible frameworks such as Co(bdp) for gas separation applications.

Differential Enthalpy of CO_2 versus CH_4 Adsorption. A more quantitative comparison of the energetic favorability of a CO_2-templated pore compared to a CH_4-templated pore can be made by examining the differential enthalpy of adsorption (h_{ads}) for each gas within Co(bdp). To determine h_{ads} of CO_2 adsorption, CO_2 adsorption isotherms were collected across a range of temperatures (Figure 4a; isotherm interpolation and h_{ads} calculations are described in the Supporting Information). Similar to the data previously reported for CH_4,[7c] a plot of the differential enthalpies of CO_2 adsorption reveals significant reductions in the amount of heat released upon CO_2 adsorption during the discrete, endothermic structural phase changes relative to the regions between these phase changes (Figure 4b). For comparison, the isostructural metal−organic frameworks Ni(bdp) and Zn(bdp), which retain their

DOI: 10.1021/jacs.8b06062
J. Am. Chem. Soc. 2018, 140, 10324−10331

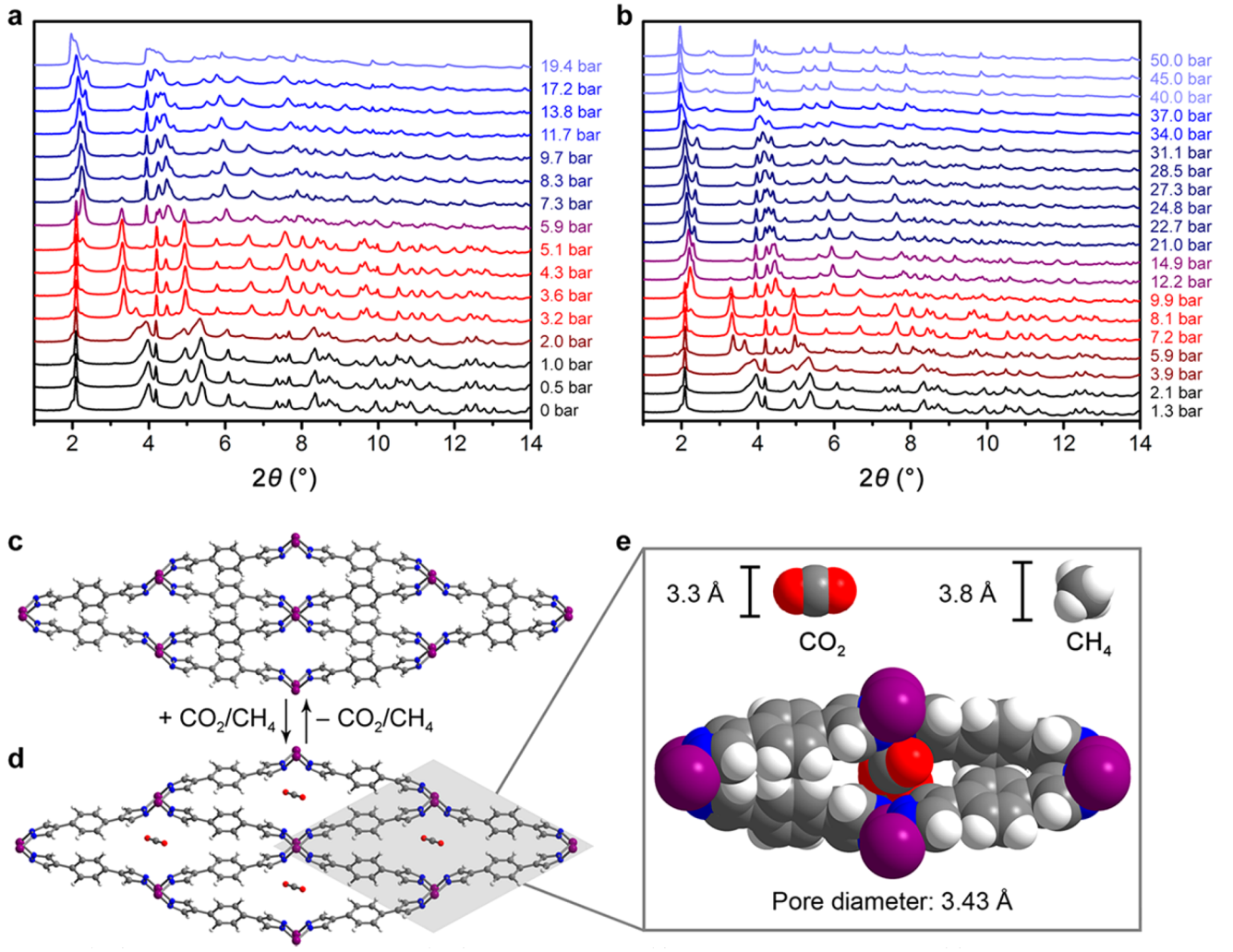

Figure 3. (a, b) Powder X-ray diffraction data for Co(bdp) dosed with pure CO_2 (a) and a 50:50 mixture of CO_2/CH_4 (b) over a range of pressures. In both data sets, the abrupt appearance or disappearance of peaks indicates discrete phase changes, whereas gradually shifting peaks indicate framework breathing. Colors are for clarity only. All data were collected at λ = 0.45336 Å and 25 °C. (c, d) Both pure CO_2 at 3.6 bar and a 50:50 CO_2/CH_4 mixture at 7.2 bar induce a structural change in Co(bdp), resulting in an expansion of the one-dimensional channels of the collapsed framework (c) to an aperture ideally sized to adsorb CO_2 and exclude CH_4 (d). Gray, blue, white, purple, and red spheres represent C, N, H, Co, and O atoms, respectively. (e) The pore diameter of 3.43 Å refers to the distance between opposing N atoms across the one-dimensional channel (in the collapsed phase, this distance is 1.55 Å). The kinetic diameters of CO_2 and CH_4 (3.3 and 3.8 Å, respectively) are shown for comparison.

expanded framework structures upon desolvation and do not exhibit flexibility, both display differential enthalpies of CO_2 adsorption of −20 kJ/mol at zero coverage.[21] Notably, these h_{ads} values are very close to those observed for Co(bdp) between its CO_2-induced phase changes. During the first phase change, Co(bdp) shows h_{ads} values in the range −24 to −26 kJ/mol, which are significantly lower in magnitude than what might be expected, given that each CO_2 molecule is tightly enclathrated within the framework (Figure 3d,e). During the second and third CO_2-induced phase changes, the magnitude of h_{ads} plummets dramatically, reaching values as small as −11 and −16 kJ/mol, respectively. Thus, the structural phase changes of Co(bdp) both give rise to selective CO_2 adsorption and, because of their endothermic nature, can also serve to substantially mitigate the amount of heat that must be dissipated during adsorption.

It is important to note that the differential enthalpy of adsorption for CH_4 in Co(bdp) is much lower than that for CO_2, varying from −8 kJ/mol during the first phase change to −14 kJ/mol after the phase change.[7c] Therefore, it is much more enthalpically favorable for Co(bdp) to adopt a pure-CO_2 phase rather than to adopt a pure-CH_4 phase, or even to replace some of the adsorbed CO_2 molecules with CH_4 to form a mixed CO_2/CH_4 phase. We hypothesize that it is this enthalpy difference that leads to the CO_2/CH_4 selectivity observed in Co(bdp), and that this effect may extend to other metal−organic frameworks capable of expanding continuously from a nonporous evacuated structure to a large-pore structure that would not otherwise be expected to exhibit selective adsorption via size exclusion.

CO_2/CH_4 Selectivity under a CH_4-Rich Atmosphere. Although the adsorption of CO_2 in Co(bdp) is enthalpically favored over CH_4 for an ∼50:50 ratio of the two gases, we wanted to probe whether the near-perfect selectivity persisted under a radically different gas ratio. To this end, the framework was exposed to equilibrium pressures of 3.7 bar of CO_2 and 54.9 bar of CH_4, representing a 6:94 molar ratio of CO_2/CH_4. Under these conditions, we found that although the material

DOI: 10.1021/jacs.8b06062
J. Am. Chem. Soc. 2018, 140, 10324−10331

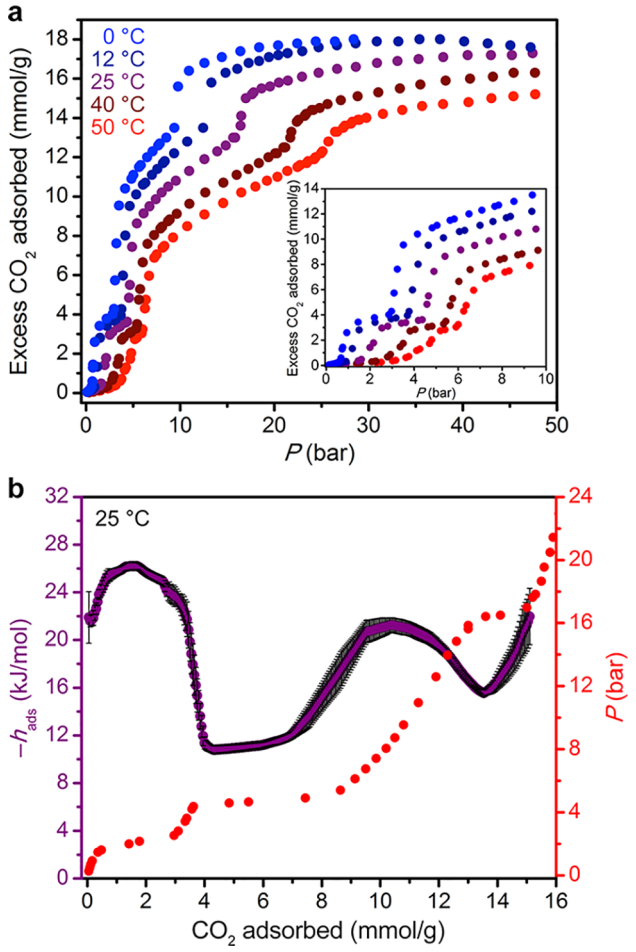

Figure 4. (a) Variable-temperature CO_2 adsorption data for Co(bdp). Minor changes in temperature move the pressure at which the CO_2-induced phase changes occur, offering a straightforward way to tailor the step pressure to a desired set of separation conditions. (b) Differential enthalpies (h_{ads}) of CO_2 adsorption in Co(bdp) are shown in purple (standard errors are shown as black bars) as a function of CO_2 loading. Local minima in $-h_{ads}$ correspond to regions in which Co(bdp) undergoes an endothermic structural expansion, which offsets some of the heat released upon CO_2 adsorption and provides intrinsic thermal management. The single-component CO_2 adsorption isotherm (red circles) is provided for comparison.

remains selective for CO_2 (adsorbing 8.5 mmol/g), a significant amount of CH_4 (2.1 mmol/g) is also adsorbed (Figure 2b). Thus, the calculated CO_2/CH_4 selectivity is reduced to 61 ± 4 under these conditions (see Supporting Information for selectivity calculations and a discussion of error). This result highlights that even if near-perfect selectivity persists beyond several phase changes in a flexible metal–organic framework, it is not correct to assume that it will persist for all equilibrium ratios for a given gas mixture. We note, however, that the measured multicomponent selectivity for CO_2 under CH_4-rich conditions is still significantly greater than the selectivity of 5.7 calculated at the corresponding pressures from the single-component adsorption isotherms (see the Supporting Information).

Tuning the Phase-Change Pressure. To supplement the equilibrium adsorption experiments described above, the separation ability of Co(bdp) was tested under dynamic breakthrough conditions. A 50:50 mixture of CO_2/CH_4 was flowed through a column of Co(bdp) at 7 bar and 22 °C to simulate the first data point of Figure 2a, and the results of the breakthrough experiment uphold the equilibrium findings at these conditions. The material adsorbs only CO_2, with CH_4 adsorption within error of zero (see the Supporting Information for calculations and experimental details). However, because the first CO_2-induced step in the 25 °C isotherm occurs at 2 bar (Figure 1b) and Co(bdp) adsorbs no CO_2 below this pressure, a 22 °C breakthrough experiment will always allow ~2 bar of CO_2 to slip through the column, as discussed previously for flexible adsorbents.[22] Thus, the pressure of the first CO_2-induced phase change makes Co(bdp) impractical for the production of pure CH_4 under these conditions, owing to the low purity of the outlet stream.

There are several straightforward ways to improve the purity of the outlet stream. First, as seen in Figure 4a, relatively minor changes in temperature have a dramatic effect on the step pressure; for example, by reducing the temperature from 25 to 12 °C, the CO_2 pressure necessary to induce a phase change is cut in half. Alternatively, we have shown previously that fluorination of the bdp^{2-} linker can lower the CH_4-induced step pressure, as fluorine disrupts intraframework $\pi-\pi$ interactions that stabilize the collapsed phase.[7d] Indeed, fluorination of the linker lowers the first CO_2-induced step pressure from ~2 bar to ~0.6 bar (Figure 5). Finally, the wider

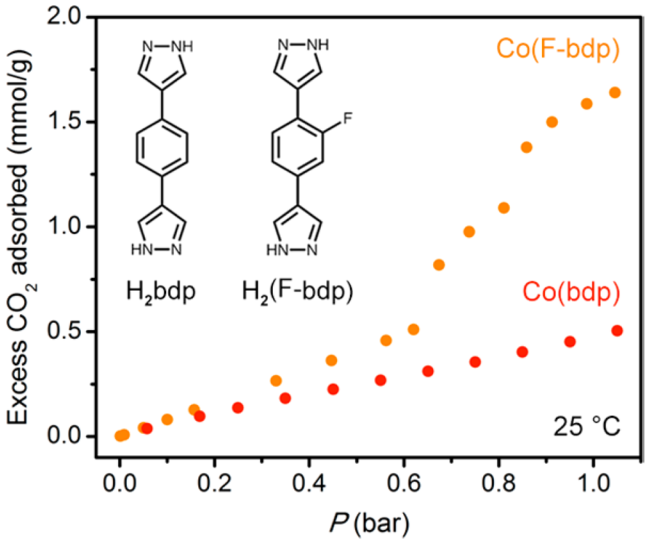

Figure 5. Low-pressure CO_2 adsorption isotherms for Co(bdp) and a fluorinated derivative, Co(F-bdp). Functionalization of the H_2bdp linker with a single fluorine atom shifts the first CO_2-induced step from ~2 bar to ~0.6 bar, providing a means of synthetic control over the adsorption and separation properties of the material.

community has identified many other flexible metal–organic frameworks with a variety of step pressures under various gases,[5] and because our findings indicate that flexible frameworks can exhibit very high inherent selectivities under equilibrium conditions, further research into the multicomponent adsorption behavior of a diverse set of flexible frameworks may ultimately make it possible to choose an adsorbent with step pressures tailored to a given separation.

CONCLUSIONS

Using multicomponent equilibrium adsorption and *in situ* powder X-ray diffraction measurements, we have demonstrated that the flexible metal–organic framework Co(bdp) achieves

DOI: 10.1021/jacs.8b06062
J. Am. Chem. Soc. 2018, 140, 10324–10331

high CO_2/CH_4 selectivity for a wide range of pressures via reversible CO_2 templating. At 7.2 bar of CO_2/CH_4 (corresponding to a CO_2 partial pressure of 3.6 bar), the diffraction results show that CO_2/CH_4 selectivity results from size exclusion, as Co(bdp) adopts a phase with a pore aperture large enough to admit CO_2 but not CH_4. At higher pressures, Co(bdp) expands to phases with larger pores capable of admitting CH_4 molecules, but the enthalpic favorability of CO_2-clathrate formation drives the continued exclusion of CH_4. For a CO_2/CH_4 ratio of 6:94 heavily favoring CH_4, however, this exceptional selectivity is diminished, indicating the importance of using multicomponent equilibrium experiments across a wide range of conditions to achieve an accurate understanding of the gas separation performance of a structurally flexible material. Finally, single-component CO_2, CH_4, N_2, and H_2 adsorption isotherms collected for Co(bdp) suggest that this material may achieve high selectivities and capacities in other important gas separations, including CO_2 from N_2, CO_2 from H_2, CH_4 from N_2, and CH_4 from H_2. Importantly, as previously demonstrated for CH_4 storage applications,[7d] adding substituents to the bdp^{2-} linkers in Co(bdp) provides a means of controlling the adsorption isotherm step pressure, which should allow these flexible adsorbents to be customized for specific separations.

■ ASSOCIATED CONTENT

Supporting Information

The Supporting Information is available free of charge on the ACS Publications website at DOI: 10.1021/jacs.8b06062.

Crystal data for Co(bdp), first CO_2-expanded phase (CIF)

Synthetic details and descriptions of crystallographic and gas adsorption data analysis (PDF)

■ AUTHOR INFORMATION

Corresponding Author

*E-mail: jrlong@berkeley.edu.

ORCID

Mercedes K. Taylor: 0000-0002-0945-766X

Jonathan E. Bachman: 0000-0002-3313-2355

Jeffrey R. Long: 0000-0002-5324-1321

Notes

The authors declare no competing financial interest.

■ ACKNOWLEDGMENTS

This research was supported by the Center for Gas Separations Relevant to Clean Energy Technologies, an Energy Frontier Research Center supported by the U.S. Department of Energy, Office of Science, Office of Basic Energy Sciences, under Award DE-SC0001015. Powder X-ray diffraction data were collected on the 17-BM-B Beamline at the Advanced Photon Source, a U.S. Department of Energy Office of Science User Facility operated by Argonne National Laboratory. Use of the Advanced Photon Source at Argonne National Laboratory was supported by the U.S. Department of Energy, Office of Science, Office of Basic Energy Sciences, under Contract No. DE-AC02-06CH11357. J.D.T. gratefully acknowledges research support from the U.S. Department of Energy, Office of Energy Efficiency and Renewable Energy, Fuel Cell Technologies Office, under Contract No. DE-AC36-08GO28308. We further thank the National Science Foundation for providing graduate fellowship support for M.K.T., J.O., and J.A.M.; Dr. Miguel I. Gonzalez, Dr. Matthew T. Kapelewski, and Dr. C. Michael McGuirk for helpful discussions and experimental assistance; and Dr. Katie R. Meihaus for editorial assistance.

■ REFERENCES

(1) Sholl, D. S.; Lively, R. P. *Nature* **2016**, *532*, 435.

(2) (a) Zhang, Y.; Sunarso, J.; Liu, S.; Wang, R. *Int. J. Greenhouse Gas Control* **2013**, *12*, 84. (b) Service, R. F. *Science* **2014**, *346*, 538.

(3) Rufford, T. E.; Smart, S.; Watson, G. C. Y.; Graham, B. F.; Boxall, J.; Diniz da Costa, J. C.; May, E. F. *J. Pet. Sci. Eng.* **2012**, *94–95*, 123.

(4) (a) Li, J.-R.; Kuppler, R. J.; Zhou, H.-C. *Chem. Soc. Rev.* **2009**, *38*, 1477. (b) Yu, J.; Xie, L.-H.; Li, J.-R.; Ma, Y.; Seminario, J. M.; Balbuena, P. B. *Chem. Rev.* **2017**, *117*, 9674.

(5) (a) Horike, S.; Shimomura, S.; Kitagawa, S. *Nat. Chem.* **2009**, *1*, 695. (b) Schneemann, A.; Bon, V.; Schwedler, I.; Senkovska, I.; Kaskel, S.; Fischer, R. A. *Chem. Soc. Rev.* **2014**, *43*, 6062. (c) Elsaidi, S. K.; Mohamed, M. H.; Banerjee, D.; Thallapally, P. K. *Coord. Chem. Rev.* **2018**, *358*, 125.

(6) (a) Thallapally, P. K.; Tian, J.; Kishan, M. R.; Fernandez, C. A.; Dalgarno, S. J.; McGrail, P. B.; Warren, J. E.; Atwood, J. L. *J. Am. Chem. Soc.* **2008**, *130*, 16842. (b) Choi, H.-S.; Suh, M. P. *Angew. Chem., Int. Ed.* **2009**, *48*, 6865. (c) Couck, S.; Denayer, J. F. M.; Baron, G. V.; Remy, T.; Gascon, J.; Kapteijn, F. *J. Am. Chem. Soc.* **2009**, *131*, 6326. (d) Hamon, L.; Llewellyn, P. L.; Devic, T.; Ghoufi, A.; Clet, G.; Guillerm, V.; Pirngruber, G. D.; Maurin, G.; Serre, C.; Driver, G.; van Beek, W.; Jolimaître, E.; Vimont, A.; Daturi, M.; Férey, G. *J. Am. Chem. Soc.* **2009**, *131*, 17490. (e) Kanoh, H.; Kondo, A.; Noguchi, H.; Kajiro, H.; Tohdoh, A.; Hattori, Y.; Xu, W.-C.; Inoue, M.; Sugiura, T.; Morita, K.; Tanaka, H.; Ohba, T.; Kaneko, K. *J. Colloid Interface Sci.* **2009**, *334*, 1. (f) Fernandez, C. A.; Thallapally, P. K.; Motkuri, R. K.; Nune, S. K.; Sumrak, J. C.; Tian, J.; Liu, J. *Cryst. Growth Des.* **2010**, *10*, 1037. (g) Inubushi, Y.; Horike, S.; Fukushima, T.; Akiyama, G.; Matsuda, R.; Kitagawa, S. *Chem. Commun.* **2010**, *46*, 9229. (h) Kishan, M. R.; Tian, J.; Thallapally, P. K.; Fernandez, C. A.; Dalgarno, S. J.; Warren, J. E.; McGrail, B. P.; Atwood, J. L. *Chem. Commun.* **2010**, *46*, 538. (i) Nakagawa, K.; Tanaka, D.; Horike, S.; Shimomura, S.; Higuchi, M.; Kitagawa, S. *Chem. Commun.* **2010**, *46*, 4258. (j) Wu, H.; Reali, R. S.; Smith, D. A.; Trachtenberg, M. C.; Li, J. *Chem. - Eur. J.* **2010**, *16*, 13951. (k) Zhang, J.; Wu, H.; Emge, T. J.; Li, J. *Chem. Commun.* **2010**, *46*, 9152. (l) Kauffman, K. L.; Culp, J. F.; Allen, A. J.; Espinal, L.; Wong-Ng, W.; Brown, T. D.; Goodman, A.; Bernardo, M. P.; Pancoast, R. J.; Chirdon, D.; Matranga, C. *Angew. Chem., Int. Ed.* **2011**, *50*, 10888. (m) Xiang, S.-C.; Zhang, Z.; Zhao, C.-G.; Hong, K.; Zhao, X.; Ding, D.-R.; Xie, M.-H.; Wu, C.-D.; Das, M. C.; Gill, R.; Thomas, K. M.; Chen, B. *Nat. Commun.* **2011**, *2*, 204. (n) Horike, S.; Inubushi, Y.; Hori, T.; Fukushima, T.; Kitagawa, S. *Chem. Sci.* **2012**, *3*, 116. (o) Liao, P. Q.; Zhou, D.-D.; Zhu, A.-X.; Jiang, L.; Lin, R.-B.; Zhang, J.-P.; Chen, X.-M. *J. Am. Chem. Soc.* **2012**, *134*, 17380. (p) Nijem, N.; Wu, H.; Canepa, P.; Marti, A.; Balkus, K. J., Jr.; Thonhauser, T.; Li, J.; Chabal, Y. J. *J. Am. Chem. Soc.* **2012**, *134*, 15201. (q) Yuan, B.; Ma, D.; Wang, X.; Li, Z.; Li, Y.; Liu, H.; He, D. *Chem. Commun.* **2012**, *48*, 1135. (r) Lin, Z.-J.; Huang, Y.-B.; Liu, T.-F.; Li, X.-Y.; Cao, R. *Inorg. Chem.* **2013**, *52*, 3127. (s) Sato, H.; Kosaka, W.; Matsuda, R.; Hori, A.; Hijikata, Y.; Belosludov, R. V.; Sakaki, S.; Takata, M.; Kitagawa, S. *Science* **2014**, *343*, 167. (t) Chen, D.-M.; Zhang, X.-P.; Shi, W.; Cheng, P. *Inorg. Chem.* **2015**, *54*, 5512. (u) Li, L.; Wang, Y.; Yang, J.; Wang, X.; Li, J. *J. Mater. Chem. A* **2015**, *3*, 22574. (v) Foo, M. L.; Matsuda, R.; Hijikata, Y.; Krishna, R.; Sato, H.; Horike, S.; Hori, A.; Duan, J.; Sato, Y.; Kubota, Y.; Takata, M.; Kitagawa, S. *J. Am. Chem. Soc.* **2016**, *138*, 3022. (w) Zhao, Y.-P.; Li, Y.; Cui, C.-Y.; Xiao, Y.; Li, R.; Wang, S.-H.; Zheng, F.-K.; Guo, G.-C. *Inorg. Chem.* **2016**, *55*, 7335. (x) Carrington, E. J.; McAnally, C. A.; Fletcher, A. J.; Thompson, S. P.; Warren, M.; Brammer, L. *Nat. Chem.* **2017**, *9*, 882. (y) Hiraide, S.; Tanaka, H.; Ishikawa, N.; Miyahara, M. T. *ACS Appl. Mater. Interfaces* **2017**, *9*, 41066. (z) Wang, H.; Cao, H.;

DOI: 10.1021/jacs.8b06062
J. Am. Chem. Soc. 2018, 140, 10324–10331

Zheng, J.-J.; Mathew, S.; Hosono, H.; Zhou, B.; Lyu, H.; Kusaka, S.; Jin, W.; Kitagawa, S.; Duan, J. *Chem. - Eur. J.* **2018**, *24*, 6412.
(7) (a) Choi, H. J.; Dincă, M.; Long, J. R. *J. Am. Chem. Soc.* **2008**, *130*, 7848. (b) Herm, Z. R.; Swisher, J. A.; Smit, B.; Krishna, R.; Long, J. R. *J. Am. Chem. Soc.* **2011**, *133*, 5664. (c) Mason, J. A.; Oktawiec, J.; Taylor, M. K.; Hudson, M. R.; Rodriguez, J.; Bachman, J. E.; Gonzalez, M. I.; Cervellino, A.; Guagliardi, A.; Brown, C. M.; Llewellyn, P. L.; Masciocchi, N.; Long, J. R. *Nature* **2015**, *527*, 357. (d) Taylor, M. K.; Runčevski, T.; Oktawiec, J.; Gonzalez, M. I.; Siegelman, R. L.; Mason, J. A.; Ye, J.; Brown, C. M.; Long, J. R. *J. Am. Chem. Soc.* **2016**, *138*, 15019.
(8) Mason, J. A.; Veenstra, M.; Long, J. R. *Chem. Sci.* **2014**, *5*, 32.
(9) Lemmon, E. W.; Huber, M. L.; McLinden, M. O. *NIST Standard Reference Database 23: Reference Fluid Thermodynamic and Transport Properties REFPROP Version 8.0*; National Institute of Standards and Technology: Gaithersburg, MD, 2007.
(10) Coudert, F.-X.; Jeffroy, M.; Fuchs, A. H.; Boutin, A.; Mellot-Draznieks, C. *J. Am. Chem. Soc.* **2008**, *130*, 14294.
(11) Saha, D.; Grappe, H. A.; Chakraborty, A.; Orkoulas, G. *Chem. Rev.* **2016**, *116*, 11436.
(12) Saeidi, S.; Fazlollahi, F.; Najari, S.; Iranshahi, D.; Klemeš, J. J.; Baxter, L. L. *J. Ind. Eng. Chem.* **2017**, *49*, 1.
(13) Abatzoglou, N.; Boivin, S. *Biofuels, Bioprod. Biorefin.* **2009**, *3*, 42.
(14) Zhang, Z.; Yao, Z.-Z.; Xiang, S.; Chen, B. *Energy Environ. Sci.* **2014**, *7*, 2868.
(15) Myers, A. L.; Prausnitz, J. M. *AIChE J.* **1965**, *11*, 121.
(16) Coudert, F.-X.; Mellot-Draznieks, C.; Fuchs, A. H.; Boutin, A. *J. Am. Chem. Soc.* **2009**, *131*, 11329.
(17) (a) Sircar, S. *Ind. Eng. Chem. Res.* **2006**, *45*, 5435. (b) Broom, D. P.; Thomas, K. M. *MRS Bull.* **2013**, *38*, 412.
(18) Rajendran, A.; Kariwala, V.; Farooq, S. *Chem. Eng. Sci.* **2008**, *63*, 2696.
(19) Mason, J. A.; McDonald, T. M.; Bae, T.-H.; Bachman, J. E.; Sumida, K.; Dutton, J. J.; Kaye, S. S.; Long, J. R. *J. Am. Chem. Soc.* **2015**, *137*, 4787.
(20) Li, B.; Cui, X.; O'Nolan, D.; Wen, H.-M.; Jiang, M.; Krishna, R.; Wu, H.; Lin, R.-B.; Chen, Y.-S.; Yuan, D.; Xing, H.; Zhou, W.; Ren, Q.; Qian, G.; Zaworotko, M. J.; Chen, B. *Adv. Mater.* **2017**, *29*, 1704210.
(21) Colombo, V.; Montoro, C.; Maspero, A.; Palmisano, G.; Masciocchi, N.; Galli, S.; Barea, E.; Navarro, J. A. R. *J. Am. Chem. Soc.* **2012**, *134*, 12830.
(22) Sotomayor, F. J.; Lastoskie, C. M. *Langmuir* **2017**, *33*, 11670.

DOI: 10.1021/jacs.8b06062
J. Am. Chem. Soc. 2018, 140, 10324−10331